



Evolution and drivers of the large-scale surface freeze-back onset in Siberian permafrost regions with the ERA5-Land reanalysis

Cécile Osy¹, Sophie Opfergelt², Arsène Druel³, François Massonnet¹

¹Earth and Climate Research Center, Earth and Life Institute, Université catholique de Louvain, Louvain-la-Neuve, 1348 Belgium

²Environmental Sciences, Earth and Life Institute, Université catholique de Louvain, Louvain-la-Neuve, 1348 Belgium

³Ecologie des Forêts Méditerranéennes (URFM), INRAe, Avignon, 84000 France

Correspondence to: François Massonnet (francois.massonnet@uclouvain.be)

Abstract. Permafrost is a defining feature of the Arctic and sub-Arctic environments. The extent of the permafrost region accounts for about a quarter of the Northern Hemisphere's terrestrial surface. While most research on permafrost has focused on the summer season—when the active layer is thawed and carbon emissions peak—the late shoulder season, marking the transition season between summer and winter and ending by surface freeze-back at the large scale, has received less attention. Yet, about 14% of the annual mean methane emissions from the permafrost occur during the refreezing period of the active layer. Understanding the seasonality, interannual variability and long-term trends of the surface freeze-back is therefore crucial to better constrain the high-latitude atmospheric carbon budget and improve Earth System Model projections. In this study, we analyze the evolution of surface freeze-back onset from 1950 to 2020 using the ERA5-Land reanalysis (0.1° spatial resolution) over a large region of Siberia encompassing the four main permafrost types. We find that surface freeze-back onset has been delayed by five days on average over that 70-yr period. Through spatial regression modeling, we show that, while several climatic and geographic factors influence freeze-back timing, the driving factor at the large scale (~kilometers) is the date when the 2-meter air temperature first falls below 0°C, followed by the snow cover depth. These findings complement previous research that focused on the small scale (~meters), which emphasized the importance of the vegetation type and the snow cover characteristics at these spatial scales. Our results provide new insights into changes during the late shoulder season in one of the world's fastest-warming regions and identify key variables to monitor for improving sub-seasonal forecasts that could become relevant to infrastructure upgrade and logistics planning in permafrost-affected areas.

1 Introduction

The region of permafrost—ground that remains at or below 0°C for at least two consecutive years—covers about one quarter of the land surface in the Northern Hemisphere (Zhang et al., 2000; Cohen et al., 2020; Obu, 2021). Permafrost stores approximately twice as much carbon as is currently present in the atmosphere, i.e., an estimated 1400-1600 GtC (Canadell et al., 2021). In the Arctic region, where air temperatures have been rising two to four times the global average—a



phenomenon known as Arctic amplification (Pithan and Mauritsen, 2014; Overland et al., 2014; Rantanen et al., 2022)—significant increases in permafrost temperatures have been recorded in the upper 30 m over the past three to four decades (Gulev et al., 2021). Moreover, under current emission scenarios, the extent of near-surface (3–4 m) permafrost is expected to decline by 24–69% relative to the 1986–2005 average value (Pörtner et al., 2019) and could even decline by 90% for high-end emission scenarios (Guo et al., 2023). It is also estimated that the annual mean frozen volume in the top 2 m of soil could shrink by 10–40% per degree of global warming (Caretta et al., 2022).

As permafrost warms and eventually thaws, it exposes previously frozen organic carbon to microbial decomposition, which in turn releases carbon in the form of carbon dioxide (CO₂) or methane (CH₄) depending on whether local conditions are aerobic or anaerobic (Schuur et al., 2008). The emission of these two potent greenhouse gases induces a positive radiative forcing on the Earth's energy balance that eventually leads to more surface warming and further permafrost thaw—a self-reinforcing process known as the permafrost-carbon feedback (Schaefer et al., 2014; Schuur et al., 2018). While the positive permafrost-carbon feedback has been identified as key element in a potential tipping point involving the permafrost, there is currently no evidence of an acceleration of permafrost thaw at the large-scale and the relationship between permafrost area and global mean temperature remains close to linear (Nitzbon et al., 2024).

At the seasonal scale, permafrost carbon emissions peak during the summer when soil temperatures are highest, although microbial decomposition—and the resulting release of CO₂ and CH₄—can continue even under cold conditions (Elberling and Brandt, 2003; Miner et al., 2022). The late shoulder season (the period starting after plant senescence and ending by surface freeze-back; Fig. 1) deserves particular attention for two reasons. First, its end determines the refreezing of the active layer which accounts for a non-negligible 14% of the annual mean CH₄ emissions (Rößger et al., 2022). Second, it coincides with the seasonal peak of Arctic amplification, as air and ground temperatures have been observed to rise most rapidly from late summer to early winter (Huang, 2017; Rantanen et al., 2022). As a result, accurately identifying the onset of surface freeze-back—and how it evolves in a warming climate—is key to understanding the seasonality of permafrost carbon emissions in present and future conditions.

With the many observed shifts in Arctic climate indicators, it is reasonable to hypothesize that the onset of the surface freeze-back has also undergone significant changes. However, fine-scale observations in permafrost-covered regions—typically collected at meter-scale resolution (e.g., Siewert et al., 2021)—lack the spatial coverage needed to determine whether local changes also occur at broader spatial scales, on the order of kilometers. Moreover, long-term and temporally consistent datasets suitable for climate-scale analyses remain scarce or altogether absent. Consequently, the evolution of the onset of surface freeze-back remains poorly documented and has yet to be comprehensively characterized or quantified. In addition, permafrost studies exhibit a strong seasonal bias, with far more observations collected between June and August than during the transitional (spring and autumn) and cold (winter) seasons, primarily due to accessibility constraints (Shogren et al., 2020; Rößger et al., 2022). While year-round ground temperature time series exist at several monitoring sites

(e.g., Romanovsky et al., 2007; Batir et al., 2017; Smith et al., 2022), their localized nature limits their representativeness for broader regions. Consequently, no robust conclusions can yet be drawn about long-term trends in the timing of freeze-back at interannual or interdecadal time scales across large spatial domains.

Several knowledge gaps and research questions thus remain open: What is the year-to-year variability in the onset of surface freeze-back? Are long-term trends detectable? Can these trends be linked to specific climatic and geographic contexts? These questions form the backbone of this study. The specific objectives of this work are (i) to investigate the evolution of the onset of surface freeze-back over the past 70 years and (ii) to identify the main drivers of observed changes and quantify their relative contributions. In the following section (Section 2: Methodology), we review the datasets, variables, study area and statistical models used to address these questions. We then present the trends in the onset of surface freeze-back and their relationship with key variables (Section 3: Results). We discuss the limitations of the study in Section 4 (Discussion) before concluding (Section 5: Conclusion).

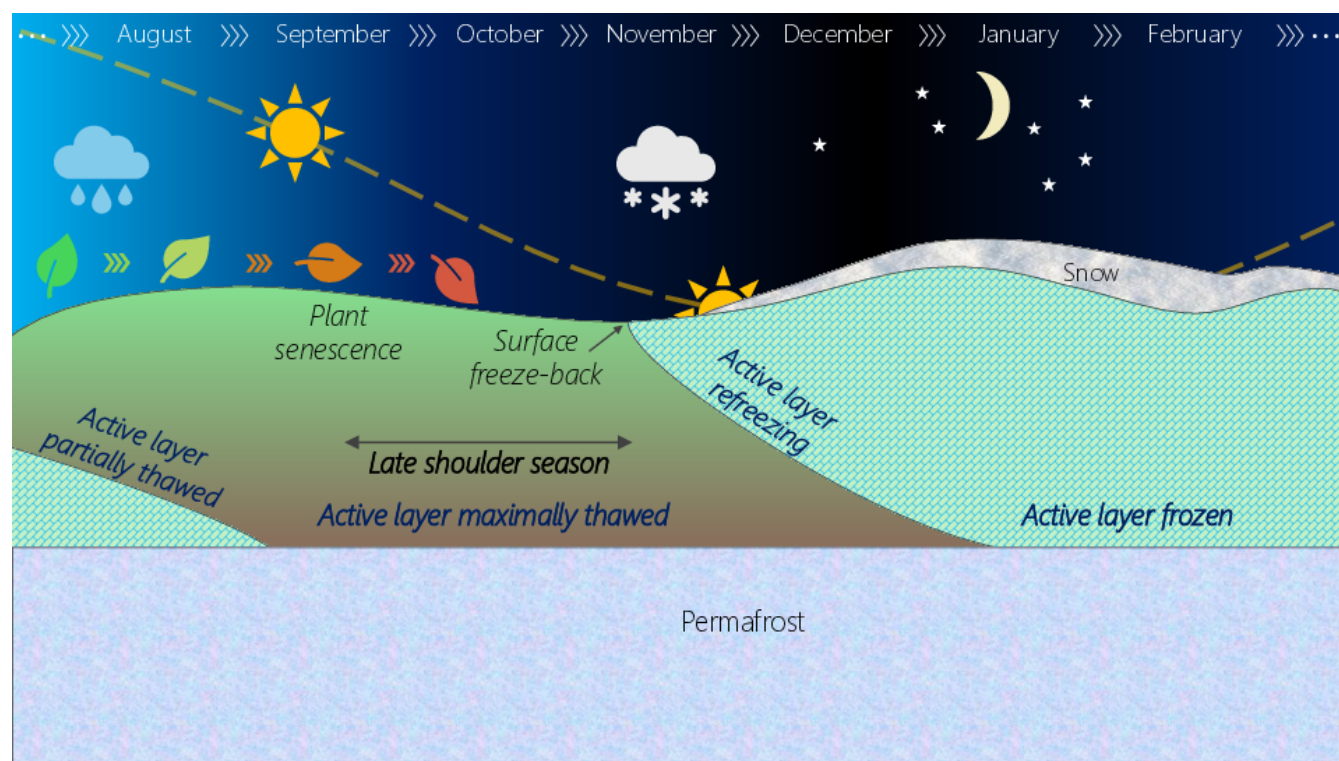


Figure 1: Conceptual scheme of the seasonal transition between summer and winter with the late shoulder season marking the transition between plant senescence and surface freeze-back, and the activer layer refreezing period. Note that the figure is not to scale and misses many characteristics such as the seasonality of methane fluxes.

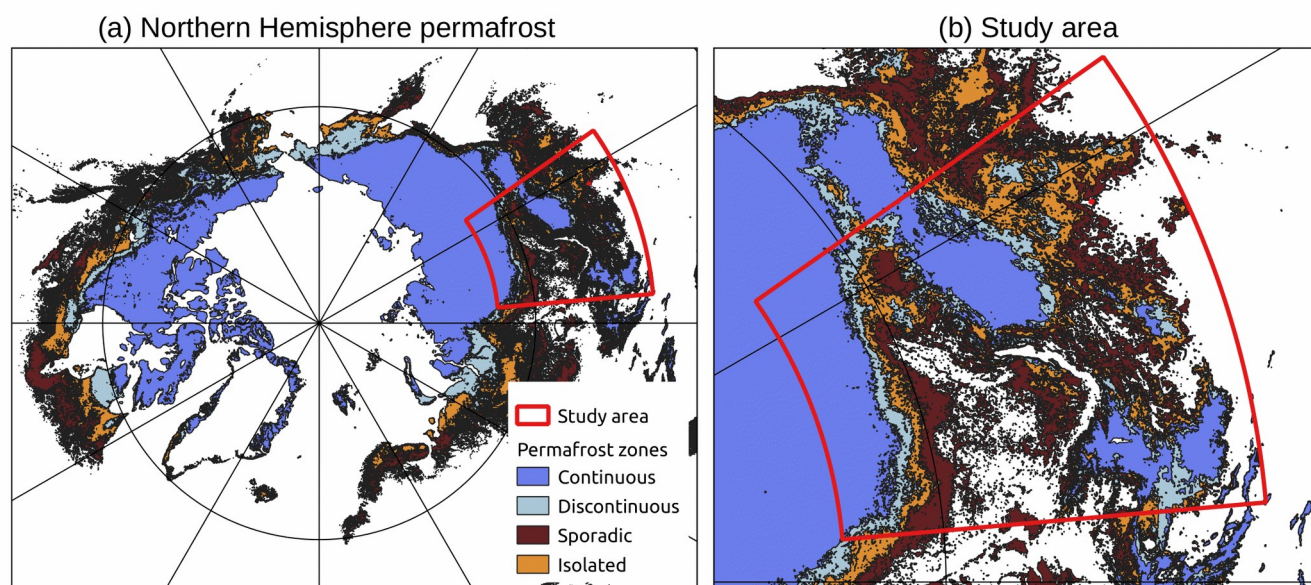


80 2 Methodology

2.1 Study area

The study area (45-65°N; 95-125°E) is located in Siberia, Russia (Fig. 2). It covers approximately 4.2 million km² and encompasses all four main permafrost zones, classified by the proportion of the ground underlain by permafrost: continuous (> 90%), discontinuous (50-90 %), sporadic (10-50%), and isolated (< 10%), following the dataset of Obu et al. (2018)

85 which maps permafrost extent across the Northern Hemisphere at 1 km resolution for the period 2000–2016. The broad spatial coverage ensures sufficient sampling across all zones to support statistically robust conclusions.



90 **Figure 2: Maps of (a) the Northern Hemisphere and (b) the study area highlighting the four different permafrost zones defined following the classification of Obu et al., 2018).**

2.2 ERA5-Land

This study employs the ERA5-Land dataset (Muñoz-Sabater et al., 2021) as the primary source of information to address the research questions outlined in the introduction. ERA5-Land is the land component of the fifth-generation European ReAnalysis (ERA5; Hersbach et al., 2020) produced by the European Centre for Medium-Range Weather Forecasts

95 (ECMWF). It provides high-frequency (1-hr), global, high resolution (~9 km) data generated by numerical integrations of



ECMWF's land surface model (the Carbon-Hydrology-Tiled ECMWF Scheme for Surface Exchanges over Land; CHTESSEL). The land surface model is driven by downscaled atmospheric forcing derived from the ERA5 reanalysis. While ERA5-Land does not assimilate land observations directly, the land surface evolution is indirectly influenced by observations through the atmospheric forcing. The near-surface thermodynamic fields are also corrected for ground
100 elevation. The dataset is available from 1950 to present.

The CHTESSEL model used in ERA5-Land solves energy and mass conservation equations to prognostically calculate key land state variables, including soil temperature and snow cover. Compared to earlier model versions, ERA5-Land accounts for more comprehensive snow-related processes, such as changes in density due to overburden and thermal metamorphism, which eventually affects the snow cover fraction (Cao et al., 2020). Soil heat fluxes are modeled by Fourier's law and the
105 soil column is discretized into four layers: 0-7 cm, 7-28 cm, 28-100cm, 100-289 cm. Vegetation and land surface characteristics are prescribed as time-invariant fields, meaning that soil type, vegetation type and vegetation cover are based on annually repeating climatologies (Muñoz-Sabater et al., 2021).

The choice of ERA5-Land dataset for this study reflects a trade-off between long-term availability, high temporal resolution, global coverage, and physical consistency. Although field observations could have offered greater realism at specific
110 locations, they lack the spatial coverage needed for robust analyses across all permafrost zones and geographical regions. Satellite remote sensing data provides broader spatial coverage but does not include all variables relevant to this study. ERA5-Land offers a good balance between these two options by proposing a consistent and comprehensive dataset. It has shown reasonable agreement with independent in-situ observations and has demonstrated improved performance over its predecessors, especially at high latitudes (Muñoz-Sabater et al., 2021). However, it is not without limitations—for example,
115 issues have been reported in hydrological modelling in the Alpine region (Dalla Torre et al., 2024) and systematic temperature biases have been identified in permafrost areas (Cao et al., 2020). We return to the limitations of ERA5-Land in the context of our research questions in Section 4 (Discussion).

2.3 Diagnosing the onset of surface freeze-back

Our diagnosis of the onset of surface freeze-back is based on the date when the daily mean ground temperature in the first
120 layer (0-7 cm) of ERA-Land drops below the 0°C threshold. Daily mean ground temperature is defined as the arithmetic average of the temperature at 00:00 and 12:00 UTC. Due to short-term meteorological fluctuations, the 0°C threshold may be crossed several times before onset of sustained winter freezing. To filter out this high-frequency variability and avoid detecting temporary freezing events, we apply a 15-day moving average (with equal weighting across days) to the daily time series. From the smoothed time series, we identify, for each grid cell and each year, the first date (counted as days elapsed
125 since July 1st) when the temperature drops below 0°C, marking the onset of persistent surface freeze-back.



The dates of surface freeze-back serve as the predictands (i.e., as our prediction targets) in our spatial prediction model developed in Section 2.4. For the trend analysis (Section 3.1), these dates are aggregated at the scale of the entire study area or by permafrost type, using area-weighted averages across all grid cells.

2.4 Spatial regression model for the onset of surface freeze-back

130 To interpret the year-to-year, long-term, and spatial variability of the onset of surface freeze-back, we use a spatial regression model. A spatial regression model is a variant of a multilinear regression model that includes an additional error structure to account for spatial autocorrelation—both among the independent variables and within the residuals. The spatial model used in this study has been implemented using the `spreg` package in Python 3.10.8 (<https://pysal.org/spreg/>). It is defined by the following two equations (Lesage and Pace, 2009):

135 $y = X\beta + e$ (1)

with

$$e = \omega Wu + \epsilon \quad (2)$$

In Equation 1, $y = (y_1, y_2, \dots, y_n)$ is an $n \times 1$ vector containing the onset dates of surface freeze-back (as defined in Section 2.3), where n is the number of grid cells in the study area. X is a $n \times m$ matrix of m independent variables (predictors, see
140 Section 2.5) of length n , each arranged in a column. β is an $m \times 1$ vector of parameters (or regression coefficients), and e is the $n \times 1$ vector representing the error term.

Equation 2 decomposes e into two components: an $n \times 1$ random vector of random errors $\epsilon = (\epsilon_1, \epsilon_2, \dots, \epsilon_n)$, and a spatially structured component ωWu . Here, ω ($n \times m$) is a spatial error coefficient, u ($m \times 1$) is the original unstructured error term, and W is the spatial weight matrix W (sparse $m \times m$ matrix) encoding the spatial structure. The suitability of a spatial error
145 model over a standard linear model was confirmed using a Lagrange multiplier test (Breusch and Pagan, 1980; Lesage and Pace, 2009), which indicated significant spatial dependence in the residuals (not shown here).

2.5 Candidate predictors

The onset of surface freeze-back depends on several factors, hereafter referred to as “predictors”, some of which are used in the spatial regression model described in the previous section. We describe below the candidate predictors considered in this
150 study, along with their data sources and post-processing steps.

2.5.1 Vegetation type



The type of vegetation is a first potential driver of the onset of surface freeze-back. Environmental stress associated with Arctic climate change has led to modifications of the Arctic flora (Beck and Goetz, 2011; Billings, 1987; Rixen et al., 2014). These modifications include widespread increases in vegetation biomass in the last decades in multiple areas across the Arctic (Beck and Goetz, 2011; Heijmans et al., 2022). Vegetation plays a key role on surface soil properties, through temperature and moisture variations. In addition, the shading caused by vegetation mitigates evaporation and therefore mitigates the risk of extreme heat events (Aalto et al., 2013; Ehrenfeld et al., 2005; Asbjornsen et al., 2011; Kropp et al., 2020). The plant canopy also modifies the local albedo and changes snow interception in winter, and thus influences the surface characteristics including its energy balances (Sturm et al., 2001b; Schuur et al., 2008; Wang et al., 2019; Druel et al., 2017).

Vegetation type data were obtained from the Global Land Cover 2000 database (Global Land Cover 2000 database, 2003) and aggregated to a 1° resolution based on the mode—the most frequently occurring vegetation type within the grid cell. Land cover types were then reclassified in three categories: “less insulating” (taller vegetation not covering the ground), “more insulating” (low-lying vegetation) and “unclassified” (Table 1). This classification is based on literature suggesting that ground-level vegetation provides greater thermal insulation than taller and sparse vegetation (Aalto et al., 2013; Kropp et al., 2020; Mamet et al., 2017; Paradis et al., 2016; Wang et al., 2019; Wynn and Mostaghimi, 2006; Wu et al., 2014). The reclassification vegetation type is included in the spatial model as a categorical (logistic) variable.

Table 1. Mapping between the vegetation type available from the Global Land Cover 2000 Database and the assigned logistic regression variable in the spatial regression model (Less insulating, more insulating, unclassified)

<i>Less insulating</i>	<i>More insulating</i>	<i>Unclassified</i>
Forest	Humid grasslands	Recent burns
Evergreen Needle-leaf	Steppe	Burns of year 2000
Deciduous Broadleaf	Palsa bog	Unclassified
Needle-leaf/Broadleaf	Riparian vegetation	
Mixed	Prostrate shrub tundra	
Broadleaf/Needle-meaf	Sedge Tundra	
Deciduous Needle-leaf	Bogs and marches	
Broadleaf deciduous shrubs	Cropland – Grassland complexes	



Forest – Natural Vegetation complexes	Croplands	
Needle-leaf evergreen shrubs	Permanent snow/ice	
Urban	Water bodies	
Barren tundra	Salt-march	
Shrub tundra		
Forest – Cropland complexes		
Bare soil and rock		

Despite some caveats, this classification offers sufficient insight to address our scientific questions. Vegetation data is only available for a single year (2000) but were used as a proxy for the entire study period (1950-2020). While we acknowledge an ongoing Arctic greening trend (Forbes et al., 2010; Myers-Smith et al., 2020), this assumption was made to focus on the spatial rather than the temporal variability of this driver.

2.5.2 Ground water content

Ground water content is a second variable that may influence the onset of the surface freeze-back by affecting heat fluxes, as it represents a source of latent energy that must be released before freezing can occur. However, ground water content is controlled by multiple factors such as precipitation (and the nature of its phase), evaporation, drainage potential and active layer thickness. Permafrost inhibits drainage, often causing perched water tables (Lawrence et al., 2015), increased surface water runoff and reduced subsurface flow (Ye et al., 2009). Changes in permafrost extent or active layer thickness—or both—can significantly alter ground hydrology (Walvoord and Krueger, 2016). Ground water content (volumetric soil water level 1 (0-7cm); variable `swv11`) was derived from the ERA5-Land dataset.

2.5.3 Snow cover

Snow cover is a third key driver of the onset of the surface freeze-back. Field studies have identified snow as a critical factor influencing permafrost dynamics (Smith et al., 2016; Morse et al., 2012; Peng et al., 2017). Due to its low thermal conductivity, snow acts as an effective insulator (Zhang et al., 2005). The timing of snowfall is particularly important: if snow accumulates early in the season, before ground temperatures drop below 0°C, it can trap heat and delay freezing; by contrast, if snowfall occurs after ground freezing, it slows further heat loss and helps maintaining cold soil conditions.

To capture the insulating effect of snow on the onset of surface freeze-back, we use the snow depth variable from ERA5-Land (variable `sd`) which provides twice-daily (00:00 and 12:00 UTC) snow depth estimates from 1950 to 2020. Based on



physical considerations, we seek to establish a critical snow depth h that would correspond to an effective insulation thickness. For this, we start from Fourier's law of heat conduction:

$$Q_{snow} = \frac{k \Delta T}{h} \quad (3)$$

195 where Q_{snow} is the conductive heat flux (W/m^2) through snow, k is the snow thermal conductivity (W/(m.K)), ΔT is the temperature difference across the snow layer, and h is the snow depth. In the absence of snow, heat transfer between the ground and the atmosphere can be approximated by the sensible heat flux:

$$Q_{no\,snow} = \rho \cdot c_{p,a} \cdot \kappa \cdot u \cdot \Delta T \quad (4)$$

200 where ρ is the air density (taken as 1.225 kg/m^3), $c_{p,a}$ is the air specific heat (taken as 1000 J/(kg.K)), κ is the coefficient of transfer (dimensionless, taken as 0.01), u is the characteristic speed of friction (taken as 3 m/s), and ΔT is the difference of temperature between the air and the ground. If we define an “insulating” snow layer as one that reduces the heat transfer to less than 5% of the value in the absence of snow: $Q_{snow}/Q_{no\,snow} < 0.05$. This implies

$$h > \frac{k}{0.05 \rho c_{p,a} \cdot \kappa \cdot u} \quad (5)$$

205 Taking $\rho_{snow} = 350 \text{ kg/m}^3$, and $k = 0.25 \text{ W/mK}$ (typical values for snow), we find that $h > 14 \text{ cm}$ corresponds to an insulating layer. This threshold is used to define the day marking the presence of snow in a grid cell (see Section 3.2).

2.5.4 Near-surface air temperature

Near-surface air temperature (hereafter referred to as “surface temperature”) plays also a direct role in the ground temperature fluctuations in the Arctic (Smith et al., 2022) and is therefore a driver of the onset of surface freeze-back. Surface temperatures are influenced by different factors (e.g., cloud cover, heat advection by dominant winds, wind-driven 210 turbulent heat fluxes at the surface) and their changes also influence other predictors (e.g., the phase of precipitation).

Surface temperature data were extracted from the ERA5-Land dataset (2-meter air temperature, variable 2t). As in Section 2.3, a 15-day moving average was applied to smooth out the high frequency variability. The 0°C threshold was then used to define the day marking the persistent cold air conditions (see Section 3.2).

2.5.5 Latitude

215 Latitude is finally an important time- variable to consider for investigating the onset of the surface freeze-back since it controls the average insolation (amount of solar energy received at the Earth's surface per unit area and per unit of time) and its seasonal distribution, which in turn influence the type of permafrost.

We note that all the variables listed above are correlated to each other (e.g., latitude correlates with near-surface temperature and snow cover) but these correlations are accommodated by the spatial regression model.

3 Results

3.1 Temporal evolution of the onset of surface freeze-back

The onset of surface freeze-back (as defined in Section 2.3) is averaged over the entire study area for each year. The resulting time series (Fig. 3) shows a significant positive trend of +4.5 days over the 1950-200 period (p-value < 0.01).

Despite this statistically significant trend, year-to-year variability remains substantial: for example, the average surface freeze-back date differed by nearly two weeks between 1967 and 1968. Additionally, the spatial averages shown in Fig. 3 mask considerable spatial variability at the grid-cell level. The ground in the grid cells situated in sporadic, isolated areas as well as the grid cells at the Southern and Western boundaries of the domain tend to freeze-back later than the average, while the areas of continuous permafrost tend to freeze-back earlier than the average (Fig. A1).

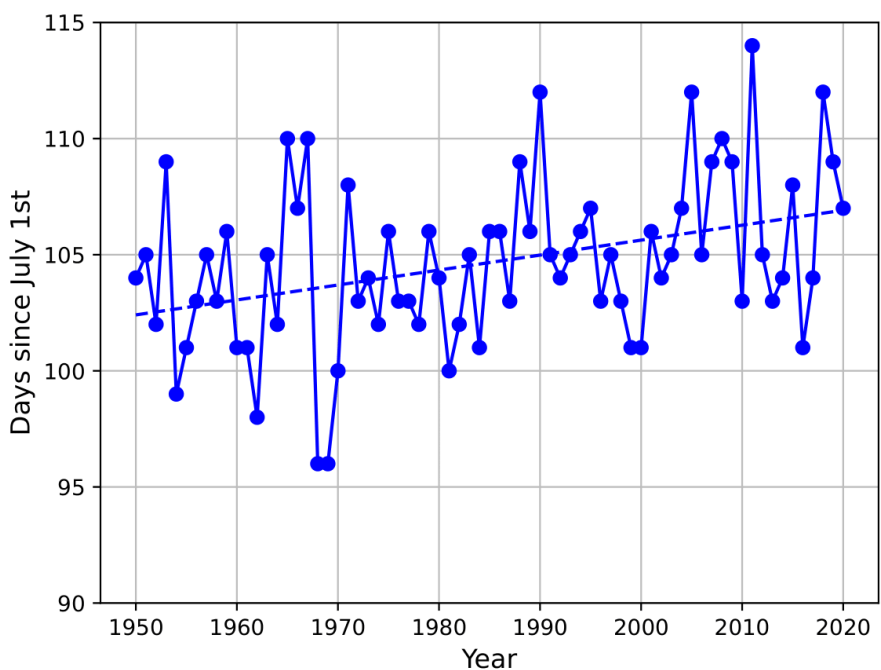


Figure 3: Evolution of the average date (counted as days since July 1st) of surface freeze-back in the study area (solid lines) and the corresponding linear trend (dashed line), according to the ERA5-Land dataset.



To further investigate regional differences and the role of spatial variability in the results, the study area was divided into four subareas corresponding to the four main permafrost zones. This allowed us to assess whether the trend reported in Fig. 3 holds within each zone individually. When calculated by permafrost zone, the positive trend in the onset of the surface freeze-back remains positive (Fig. 4). Notably, the trend is weakest in areas of continuous permafrost (+3.3 [0.4-6.3] days), which can be physically understood as follows: in these regions, ground temperatures are lower than in other regions and often well below 0°C. Ground in these regions are thus less responsive to atmospheric forcing than in other regions. In contrast, the trends in isolated (+5.1 [1.8-8.5] days), sporadic (+5.4 [2.5-8.4] days) and discontinuous (+5.2 [2.4-8.0] days) permafrost are stronger and more similar to each other in magnitude because the ground is more responsive to the atmospheric forcing. Finally, high co-variability is also noticed among the four time series of the date of surface freeze-back across the four permafrost regimes (Fig. 4). This suggests that the large-scale atmospheric drivers are the primary cause for the year-to-year variability in the surface freeze-back.

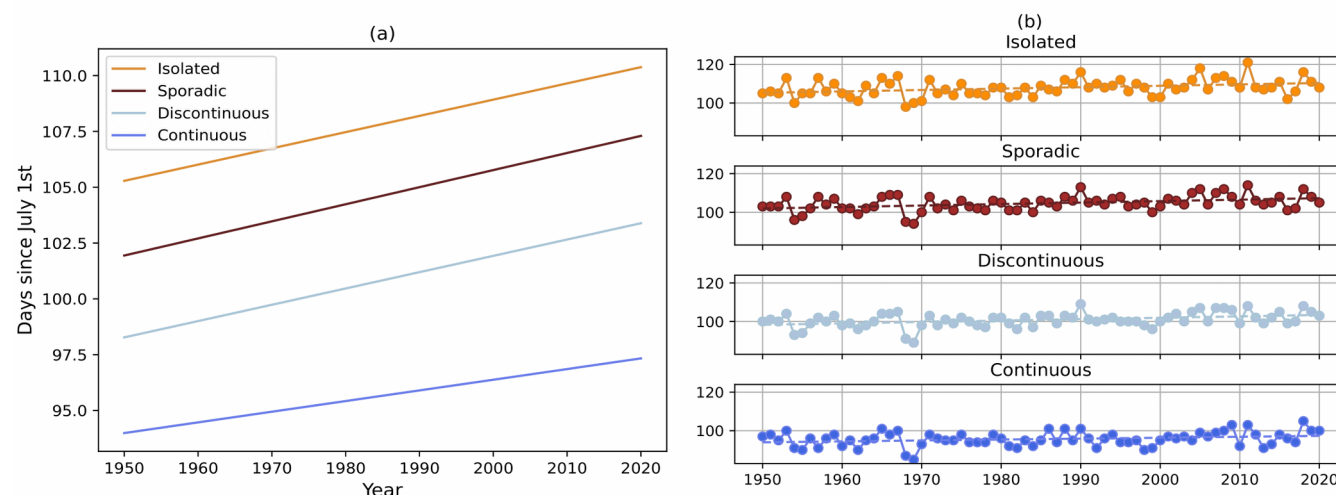


Figure 4: (a) Comparison between the trends in the onset of freeze-back (same conventions as in Fig. 2) for the trend in the day between 1950 and 2020 (p-value = 0.01 for isolated, sporadic and discontinuous permafrost; p-value = 0.03 for continuous permafrost). (b) Detailed evolution between 1950 and 2020 of the day of the onset of the surface freeze-back for the different permafrost zones. The y-axes limits are identical for easier comparison.

3.2 Drivers of the onset of surface freeze-back

The spatial regression model (Section 2.4), used to identify the key factors influencing the onset of the surface freeze-back, is applied on the candidate variables listed in Section 2.5. In contrast to the analysis of year-to-year variability of the



previous section, where the onset of surface freeze-back was averaged over space, the variables used to identify the drivers of freeze-back onset were averaged over time (1950–2020). This approach was chosen as to isolate the role of spatial variability by excluding the influence of temporal fluctuations that could have acted as a confounding factor in the analyses.

To train the spatial error model, approximately 90% of the ERA5-Land data (55,501 out of 60,501 grid cells) were randomly selected and evenly distributed across the study area. This sampling strategy preserves a portion of the data for out-of-sample model validation. The remaining dataset was used for verification, allowing for an independent assessment of model skill. Model performance was evaluated over the entire study area as well as separately for each of the four permafrost zones.

The model applied to the entire study area yields

$$day_{onset} = 0.05 - 0.08 \times day_{snow} + 1.02 \times day_{air\ temp.} \quad (6)$$

where the “day” variables are the number of days since July 1st for the onset of surface freeze-back, the snow depth exceeding 14 cm, and the air temperature dropping below 0°C, respectively. The vegetation type, ground water content (in July) and latitude were found to be non-significant covariates (p-value > 0.05) and so were not included in Eq. 6. The coefficients shown in Eq. 6 are those obtained by running the model a second time without those non-significant covariates.

To assess the predictive power of the model and to ensure it is not overfitting, we apply it to the ~10% of the data that were withheld during training. That is, we provide as input day_{snow} and $day_{air\ temp.}$ to Eq. 6 and compare the predicted values for day_{onset} to the actual values derived from ERA5-Land. The resulting scatterplot (Fig. 5) shows strong agreement between predicted and observed values, and the coefficient of determination ($R^2 = 0.78$) confirms the model’s good predictive skill.

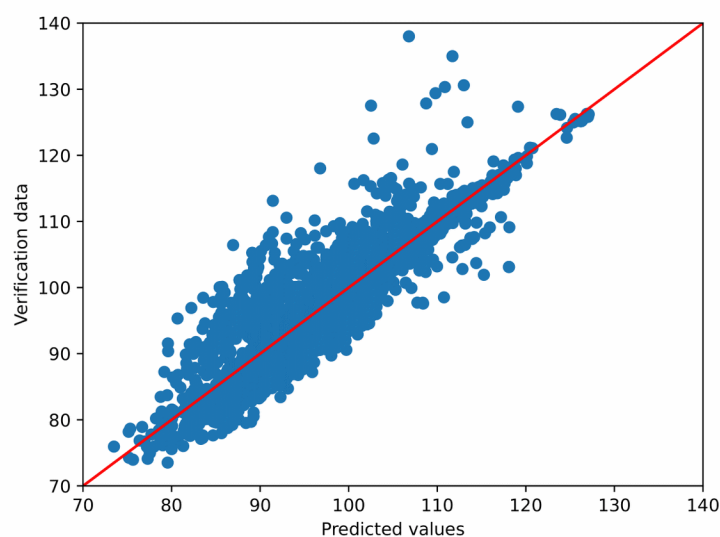




Figure 5: Predicted (x-axis, using Eq. 6) versus observed (y-axis) day of surface freeze-back in the ERA5-Land dataset (counted from July 1st).

To further investigate spatial differences, the analysis was then repeated by permafrost zone. Permafrost type is a spatially autocorrelated variable (Fig. 2) and represents a relevant predictor in its own right, as it influences key ground properties. The standardized regression equations derived for each permafrost zone are presented in Table 2. Unlike the model for the entire area, vegetation was found this time to be a significant predictor (except over continuous permafrost) of the day of surface freeze-back.

Table 2. Coefficients for the spatial regression model (Eq. 1, \hat{y}) for the different variables (X) for each permafrost zone. Latitude and ground water content were found to be systematically non-significant and hence excluded from the analysis. To ensure an easy comparison, the variables in Eq. 1 have been first standardized ((value-mean)/standard deviation).

	Constant offset	Air temperature	Snow cover	Vegetation
Isolated	0.06	0.98	-0.22	-0.07
Sporadic	0.08	1.08	-0.42	-0.06
Discontinuous	0.03	1.06	-0.53	-0.12
Continuous	0.12	0.93	-0.29	Not significant

The standardized regression equations coefficients of Table 2 reveal that both the timing of the 14 cm snow layer and the drop in 2-meter air temperature below 0°C are key predictors of surface freeze-back onset across all permafrost zones. Among these, the timing of the temperature drop consistently exhibits the largest and most significant coefficient, followed by the timing of the insulating snow cover. Vegetation is also a significant predictor in all zones except continuous permafrost where it is not significant. Both the snow and vegetation coefficients are negative, indicating that an early formation of an insulating snow cover delays the onset of surface freeze-back (as we expect), and that ground beneath insulating vegetation (e.g., grasslands) tends to freeze later in the season.

We finally repeat the scatterplot analysis for the four main zones. When analyzing the four permafrost zones separately, scatterplots comparing predicted values (from the equations in Table 2) to observed values from the verification dataset (the 10% withheld from training) show correlations ranging from 0.51 to 0.80, depending on the zone. Specifically, the



correlation coefficients are 0.76 for continuous, 0.51 for discontinuous, 0.74 for sporadic, and 0.80 for isolated permafrost
295 (Fig. 6).

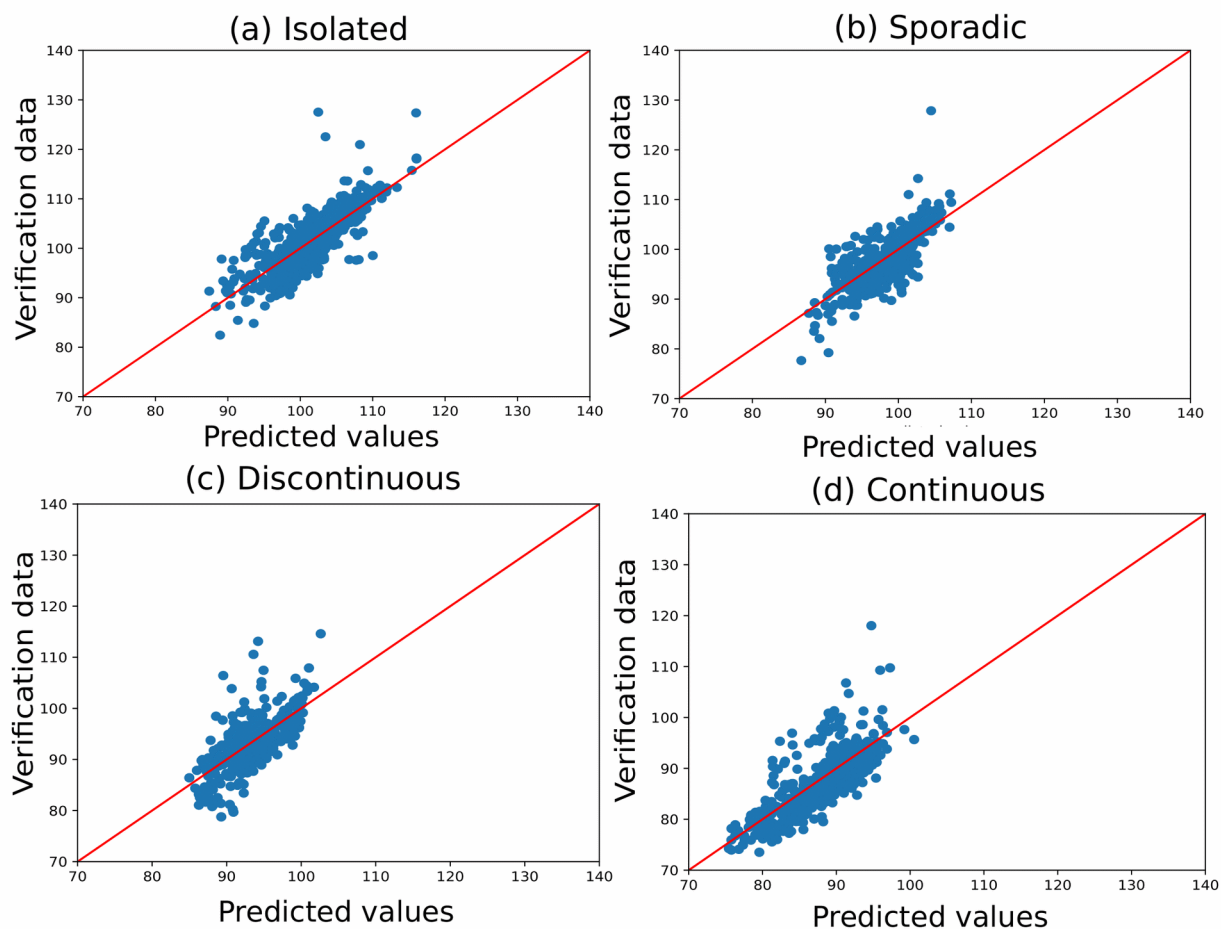


Figure 6: Predicted (with coefficients from Table 2) versus observed onset of the surface freeze-back (counted from July 1st) for (a) isolated (b) sporadic (c) discontinuous and (d) continuous permafrost zones in the study area. These scatterplots are based on the 10% of the data that was not used for training the spatial regression model.

300

4 Discussion

4.1 Surface freeze-back delayed but not equally across permafrost zones

Our results indicate that the factors controlling the onset of surface freeze-back in permafrost regions vary significantly across space. While treating the entire study area as a single unit yields more accurate predictions (in a statistical sense),



305 subdividing by permafrost zone reveals important differences in the influence of individual drivers. For instance, vegetation emerges as a significant predictor in the isolated, sporadic, and discontinuous zones, but not in the continuous permafrost zone (Table 2).

Freeze-back also occurs at different times of the year across permafrost types, with the earliest onset observed in the continuous permafrost zone (Fig. 4; Fig. A1). Between 1950 and 2020, the onset of surface freeze-back was delayed by
310 approximately 3 days in continuous permafrost areas, compared to a 5-day delay in the discontinuous, sporadic, and isolated zones (Fig. 4).

In the context of ongoing Arctic climate change and Arctic amplification, these findings suggest that ground temperature responses to key drivers of freeze-back onset evolve more rapidly in thermally marginal permafrost zones (discontinuous, sporadic, and isolated), while continuous permafrost shows a more limited shift (for now).

315 At high latitudes, where permafrost is predominantly continuous (Fig. 2), persistent winds are a well-documented feature of the environment (Wilson, 1959; Sturm et al., 2001a; Gislén et al., 2016). These strong winds contribute to highly variable snow distribution (in extent and depth), resulting in patchy snow cover across the landscape (Gislén et al., 2014; Gislén et al., 2016). Because snow is a key control on ground temperature at the field scale, this spatial variability in snow cover translates into variability in the degree of insulation it provides, and ultimately, on the variability in the date of surface
320 freeze-back. Given the strong local influence of snow on freeze-back timing, greater heterogeneity in snow cover likely leads to greater variability in the onset of surface freeze-back within the continuous permafrost zone. This spatial variability may help explain why the overall trend in freeze-back delay is weaker in continuous permafrost areas: in some locations, early freeze-back may offset later onset elsewhere, thereby dampening the overall trend signal for that permafrost zone.

4.2 Limitations of the study

325 ERA5-Land has been shown to exhibit a warm bias in high-latitude permafrost regions, particularly during winter months (Cao et al., 2020) with the strongest overestimations over Canada and Alaska. The biases over Siberia are less pronounced but regionally evident. The period analyzed in this study (July to November) is associated with smaller biases than those observed in winter. While a systematic temperature bias in ERA5-Land could affect both the estimated onset of surface freeze-back and the predictor variables used in the regression, such a bias would primarily influence absolute values—not
330 temporal trends. Therefore, while the exact dates of surface freeze-back should not be taken at face value, the trends and spatial relationships identified in this study remain robust.

At the field scale (~meters), snow cover and vegetation are widely recognized as the primary factors influencing ground temperature, largely due to their insulating properties (Luetschg et al., 2004; Zhang et al., 2001; Zhang et al., 2005; Lorant et al., 2018; Kropp et al., 2020). These factors can also be monitored via remote sensing, using indicators such as land
335 surface temperature, snow cover, and vegetation indices (Alphonse et al., 2024; Tikhomirov et al., 2021; Ylönen et al., 2025;



Beamish et al., 2020). At first glance, these findings may seem to contrast with our results, where snow cover emerges as a secondary driver after air temperature, and vegetation shows a significant impact only when the analysis is delineated by permafrost zone. This apparent discrepancy may partly arise from the overrepresentation of continuous permafrost in our study area, where vegetation has little variability and is not a significant driver. More fundamentally, the difference in spatial scale likely plays a major role. At the coarser resolution of ERA5-Land (~9 km), fine-scale heterogeneity in snow and vegetation is not fully captured, which may diminish their statistical influence on the freeze-back date. Additionally, the importance of surface temperature in our model results may indirectly reflect sub-grid variability in snow cover and vegetation, so that surface temperature would in fact act as a proxy for these unresolved processes.

4.3 Implications for permafrost and seasonally frozen regions

A delayed onset of surface freeze-back extends the window of favorable conditions for vegetation growth, potentially contributing to the observed Arctic greening (Arndt et al., 2019). In turn, increased vegetation productivity or changes in vegetation cover (Druel et al., 2019; Anderson et al., 2019) can further influence the timing of surface freeze-back. Recent studies have highlighted the complexity of vegetation–soil interactions in permafrost regions, particularly the extension of the late root growing season prior to the complete freezing of the surface soil layer (Blume-Werry et al., 2019). During this period, plants may access deeper mineral layers, promoting root development and altering nutrient cycling (Finger et al., 2016; Hewitt et al., 2018; Ogden et al., 2023). These dynamics can drive differential vegetation responses, such as increased root biomass—enhancing soil carbon storage—or even shifts in species composition (Hewitt et al., 2018; Yun et al., 2024). Such changes are further amplified by modifications in the hydrological regimes, which often accompany permafrost degradation (Finger et al., 2016; Yun et al., 2024). Altogether, shifts in freeze-back timing can trigger cascading, long-term consequences that extend beyond the growing season. These include broader impacts on surface albedo, soil structure, and ground stability—factors with important implications for Arctic ecosystem functioning and feedbacks to the climate system.

There are still large uncertainties regarding whether Arctic landscapes will become wetter or drier in the future, particularly at regional scales (Xie et al., 2015). This uncertainty has major implications for vegetation changes in the Arctic. In drier conditions, vegetation is expected to become shrub-dominated (Jónsdóttir et al., 2005; Shaver et al., 2001; Heijmans et al., 2022). Increased shrub cover, in turn, would enhance snow interception (Chapin et al., 2005; Sturm et al., 2001b), thereby altering the thermal insulation provided by snow and influencing the timing of surface freeze-back. These interactions are further complicated by feedbacks between snow cover and vegetation dynamics, making the system's evolution highly nonlinear. Establishing a robust present-day baseline for the timing and drivers of surface freeze-back was therefore a key objective of this study, providing a reference point for future modeling.

A delayed onset of surface freeze-back also favors microbial activity, thereby contributing to permafrost-derived CO₂ and CH₄ emissions (Zona et al., 2016). Although the majority of CH₄ emissions occur during the thawing season, approximately 14% of the mean annual CH₄ flux is released between the onset of surface freeze-back and the complete refreezing of the



active layer (Rößger et al., 2022). During this transitional period, parts of the soil remain unfrozen and biologically active, allowing continued microbial processes (Commane et al., 2017). Extending the window for soil biogeochemical activity during the late shoulder season—bridging the thawing and freezing periods—is also critical for the mobilization and export of dissolved organic carbon (DOC) from soils (Villani et al., 2025). Once exported to aquatic systems, this DOC becomes susceptible to microbial and photodegradation, altering the fate and persistence of carbon in the Arctic environment (Bowen et al., 2020).

4.4 Outlook

This study is primarily diagnostic, based on linear relationships established between predictor and predictand variables. However, it can serve as a foundation for predictive applications of the onset of surface freeze-back. Many weather and climate centers routinely publish seasonal forecasts of variables such as precipitation and near-surface air temperature. These forecasts, when combined and downscaled with the regression models developed in this work, could be used to produce probabilistic estimates of freeze-back onset with a lead time of several days to weeks. Although such estimates would carry uncertainties stemming from the forecast inputs, they could provide valuable information for logistical planning of field campaigns in permafrost regions. Moreover, timely knowledge of freeze-back onset could help constrain land surface models and improve representation of cold-season processes.

The predictors used in this model—air temperature, snow cover, and vegetation—are included in seasonal forecast systems, such as those from the European Centre for Medium-Range Weather Forecasts (ECMWF), making them available several months in advance. These forecasts could be used to generate probability distributions of expected freeze-back dates under current and near-future climate conditions.

Looking ahead, understanding how these key variables are projected to change can offer insights into future trends in the onset of surface freeze-back. While air temperature, snow cover, and vegetation are all expected to evolve under climate change, their trajectories will be spatially heterogeneous (Bintanja, 2018; Bjorkman et al., 2020). This suggests that future changes in freeze-back timing—and the associated permafrost carbon emissions—will also vary regionally, underlining the importance of spatially explicit projections.

5 Conclusions

The primary objective of this study was to document large-scale temporal changes in the onset of surface freeze-back across Siberian permafrost regions. Over the 70-year period from 1950 to 2020, the average onset of surface freeze-back (defined at 0–7 cm soil depth) over a 4.2 million km² area in Siberia (45–65°N, 95–125°E) has shifted by approximately five days—delaying from October 12th to October 17th.



We also investigated the drivers of this shift using a spatial error model, a type of spatial regression that accounts for spatial autocorrelation in the residuals. One of the main findings is that, at the coarse spatial scale of ERA5-Land ($\sim 0.1^\circ$ resolution), near-surface air temperature is the dominant predictor of surface freeze-back onset, followed by snow cover. This result contrasts with numerous field studies, which emphasize the roles of snow and vegetation as primary controls. This apparent discrepancy likely arises from scale differences: field studies can resolve fine-scale processes (e.g., snow interception, microtopography, vegetation heterogeneity) that are smoothed out at the coarse scale used here.

The spatial regression model was applied to both the full study area and to subsets defined by permafrost zone. While the model applied to the entire domain yielded the highest predictive accuracy ($R^2 = 0.78$), stratifying the analysis by permafrost zone provided deeper insight into how the influence of different predictors varies with permafrost type. In particular, while air temperature and snow insulation timing remained significant across all zones, vegetation insulation was only significant in the discontinuous, sporadic, and isolated permafrost zones, and not in the continuous permafrost zone. This supports the idea that the influence of vegetation is more pronounced in thermally marginal permafrost environments.

Overall, our results highlight the dominant role of air temperature in shaping freeze-back timing at large scales, with snow cover and vegetation playing secondary but still important roles. These findings reflect both the resolution of the dataset and the interdependence of variables at this scale. More broadly, they highlight how the choice of spatial scale can shape our understanding of permafrost processes. Large-scale diagnostics, such as the one presented here, complement fine-scale studies by providing an integrated perspective on regional patterns and drivers.

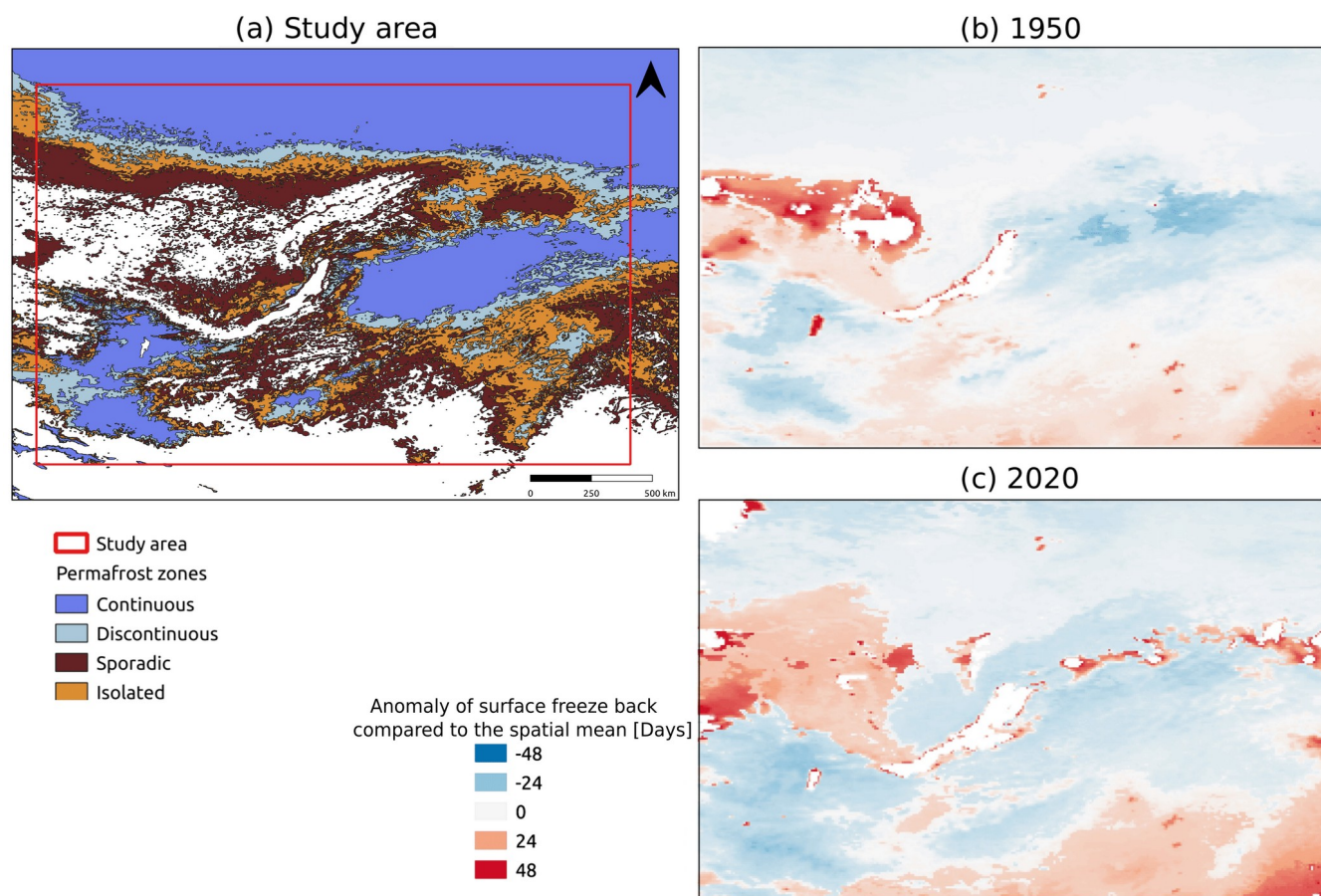


Figure A1: Study area (a) and spatial variation of the anomaly of the onset of the surface freeze-back relative to the spatial average for (b) the first year of the study (1950) and (c) the last year of the study (2020). Red areas mean that surface freeze-back occurs later than the spatial average and blue areas that surface freeze-back occurs earlier than the spatial average.

Code and data availability

The code used for this paper is available at <https://doi.org/10.5281/zenodo.14832934>

The data used is freely available online at

- "Muñoz Sabater, J. (2019): ERA5-Land hourly data from 1950 to present. Copernicus Climate Change Service (C3S) Climate Data Store (CDS). DOI: [10.24381/cds.e2161bac](https://doi.org/10.24381/cds.e2161bac)" for the ground temperature, 2m air temperature and snow data.



- "Global Land Cover 2000 database. European Commission, Joint Research Centre, 2003, <https://forobs.jrc.ec.europa.eu/glc2000>" for the vegetation data

- 430
- "Obu, Jaroslav; Westermann, Sebastian; Kääb, Andreas; Bartsch, Annett (2018): Ground Temperature Map, 2000-2016, Northern Hemisphere Permafrost [dataset]. Alfred Wegener Institute, Helmholtz Centre for Polar and Marine Research, Bremerhaven, PANGAEA, <https://doi.org/10.1594/PANGAEA.888600>" for the data on the permafrost zones.

435 **Author contributions**

CO, SO and FM took care of the conceptualization, methodology and project administration. CO conducted the analysis and wrote the manuscript with contribution from all authors. Validation was made by all authors.

Competing interests

The authors declare that they have no conflict of interest.

440 **Acknowledgements**

Cécile Osy is supported by an incentive of the Fédération Wallonie Bruxelles. François Massonnet is a F.R.S.–FNRS Research Associate, and Sophie Opfergelt is a F.R.S.–FNRS Senior Research Associate. We acknowledge that AI assistance (ChatGPT by OpenAI) was used to rephrase parts of the manuscript for readability.

References

- 445 Aalto, J., le Roux, P. C., and Luoto, M.: Vegetation Mediates Soil Temperature and Moisture in Arctic-Alpine Environments. *Arctic, Antarctic, and Alpine Research*, 45(4):429–439, 2013.

- Alphonse, A. B., Osuch, M., Wawrzyniak, T., and Hanselmann, N.: Spatio-temporal variability of surface temperatures in High Arctic periglacial environment using UAV thermal imagery and in-situ measurements, *GIScience & Remote Sensing*, 61, 2435851, <https://doi.org/10.1080/15481603.2024.2435851>, 2024.
- 450

Anderson, J. E., Douglas, T. A., Barbato, R. A., Saari, S., Edwards, J. D., and Jones, R. M.: Linking vegetation cover and seasonal thaw depths in interior Alaska permafrost terrains using remote sensing, *Remote Sensing of Environment*, 233, 111363, <https://doi.org/10.1016/j.rse.2019.111363>, 2019.

455



Arndt, K. A., Santos, M. J., Ustin, S., Davidson, S. J., Stow, D., Oechel, W. C., Tran, T. T. P., Graybill, B., and Zona, D.: Arctic greening associated with lengthening growing seasons in Northern Alaska, *Environ. Res. Lett.*, 14, 125018, <https://doi.org/10.1088/1748-9326/ab5e26>, 2019.

460 Asbjornsen, H., Goldsmith, G. R., Alvarado-Barrientos, M. S., Rebel, K., Van Osch, F. P., Rietkerk, M., Chen, J., Gotsch, S., Tobón, C., Geissert, D. R., Gómez-Tagle, A., Vache, K., and Dawson, T. E.: Ecohydrological advances and applications in plant–water relations research: a review. *Journal of Plant Ecology*, 4(1-2):3–22, 2011.

Batir, J. F., Hornbach, M. J., and Blackwell, D. D.: Ten years of measurements and modeling of soil temperature changes
465 and their effects on permafrost in Northwestern Alaska. *Global and Planetary Change*, 148:55–71, 2017.

Beamish, A., Raynolds, M. K., Epstein, H., Frost, G. V., Macander, M. J., Bergstedt, H., Bartsch, A., Kruse, S., Miles, V., Tanis, C. M., Heim, B., Fuchs, M., Chabrillat, S., Shevtsova, I., Verdonen, M., and Wagner, J.: Recent trends and remaining challenges for optical remote sensing of Arctic tundra vegetation: A review and outlook, *Remote Sensing of Environment*,
470 246, 111872, <https://doi.org/10.1016/j.rse.2020.111872>, 2020.

Beck, P. S. A. and Goetz, S. J.: Satellite observations of high northern latitude vegetation productivity changes between 1982 and 2008: ecological variability and regional differences. *Environmental Research Letters*, 6(4):045501, 2011.

475 Billings, W. D.: Constraints to Plant Growth, Reproduction, and Establishment in Arctic Environments. *Arctic and Alpine Research*, 19(4):357–365, 1987.

Bintanja, R.: The impact of Arctic warming on increased rainfall. *Scientific Reports*, Nature Publishing Group, 8(1):16001, 2018.

480



Bjorkman, A. D., García Criado, M., Myers-Smith, I. H., Ravolainen, V., Jónsdóttir, I. S., Westergaard, K. B., Lawler, J. P., Aronsson, M., Bennett, B., Gardfjell, H., Heiðmarsson, S., Stewart, L., and Normand, S.: Status and trends in Arctic vegetation: Evidence from experimental warming and long-term monitoring. *Ambio*, 49(3):678–692, 2020.

485

Blume-Werry, G., Milbau, A., Teuber, L. M., Johansson, M., and Dorrepaal, E.: Dwelling in the deep – strongly increased root growth and rooting depth enhance plant interactions with thawing permafrost soil, *New Phytologist*, 223, 1328–1339, <https://doi.org/10.1111/nph.15903>, 2019.

490 Bowen, J. C., Ward, C. P., Kling, G. W., and Cory, R. M.: Arctic Amplification of Global Warming Strengthened by Sunlight Oxidation of Permafrost Carbon to CO₂, *Geophysical Research Letters*, 47, e2020GL087085, <https://doi.org/10.1029/2020GL087085>, 2020.

Breusch, T. S. and Pagan, A. R.: The Lagrange Multiplier Test and its Applications to Model Specification in Econometrics. 495 *The Review of Economic Studies*, 47(1):239–253, 1980.

Canadell, J.G., P.M.S. Monteiro, M.H. Costa, L. Cotrim da Cunha, P.M. Cox, A.V. Eliseev, S. Henson, M. Ishii, S. Jaccard, C. Koven, A. Lohila, P.K. Patra, S. Piao, J. Rogelj, S. Syampungani, S. Zaehle, and K. Zickfeld, 2021: Global Carbon and other Biogeochemical Cycles and Feedbacks. In *Climate Change 2021: The Physical Science Basis. Contribution of 500 Working Group I to the Sixth Assessment Report of the Intergovernmental Panel on Climate Change* [Masson-Delmotte, V., P. Zhai, A. Pirani, S.L. Connors, C. Péan, S. Berger, N. Caud, Y. Chen, L. Goldfarb, M.I. Gomis, M. Huang, K. Leitzell, E. Lonnoy, J.B.R. Matthews, T.K. Maycock, T. Waterfield, O. Yelekçi, R. Yu, and B. Zhou (eds.)]. Cambridge University Press, Cambridge, United Kingdom and New York, NY, USA, pp. 673–816, 2021.

505 Cao, B., Gruber, S., Zheng, D., and Li, X.: The ERA5-Land soil temperature bias in permafrost regions. *The Cryosphere*, 14(8):2581–2595, 2020.

Caretta, M.A., A. Mukherji, M. Arfanuzzaman, R.A. Betts, A. Gelfan, Y. Hirabayashi, T.K. Lissner, J. Liu, E. Lopez Gunn, R. Morgan, S. Mwanga, and S. Supratid: Water. In: *Climate Change 2022: Impacts, Adaptation and Vulnerability. 510 Contribution of Working Group II to the Sixth Assessment Report of the Intergovernmental Panel on Climate Change* [H.-O.



Pörtner, D.C. Roberts, M. Tignor, E.S. Poloczanska, K. Mintenbeck, A. Alegría, M. Craig, S. Langsdorf, S. Löschke, V. Möller, A. Okem, B. Rama (eds.)). Cambridge University Press, Cambridge, UK and New York, NY, USA, pp. 551–712, doi:10.1017/9781009325844.006., 2022.

- 515 Chapin, F. S., Sturm, M., Serreze, M. C., McFadden, J. P., Key, J. R., Lloyd, A. H., McGuire, A. D., Rupp, T. S., Lynch, A. H., Schimel, J. P., Beringer, J., Chapman, W. L., Epstein, H. E., Euskirchen, E. S., Hinzman, L. D., Jia, G., Ping, C.-L., Tape, K. D., Thompson, C. D. C., Walker, D. A., and Welker, J. M.: Role of Land-Surface Changes in Arctic Summer Warming. *Science*, 310(5748):657–660, 2005.
- 520 Cohen, J., Zhang, X., Francis, J., Jung, T., Kwok, R., Overland, J., Ballinger, T. J., Bhatt, U. S., Chen, H. W., Coumou, D., Feldstein, S., Gu, H., Handorf, D., Henderson, G., Ionita, M., Kretschmer, M., Laliberte, F., Lee, S., Linderholm, H. W., Maslowski, W., Peings, Y., Pfeiffer, K., Rigor, I., Semmler, T., Stroeve, J., Taylor, P. C., Vavrus, S., Vihma, T., Wang, S., Wendisch, M., Wu, Y., and Yoon, J.: Divergent consensus on Arctic amplification influence on midlatitude severe winter weather. *Nature Climate Change*, 10(1):20–29, 2020.
- 525 Commane, R., Lindaas, J., Benmergui, J., Luus, K. A., Chang, R. Y.-W., Daube, B. C., Euskirchen, E. S., Henderson, J. M., Karion, A., Miller, J. B., Miller, S. M., Parazoo, N. C., Randerson, J. T., Sweeney, C., Tans, P., Thoning, K., Veraverbeke, S., Miller, C. E., and Wofsy, S. C.: Carbon dioxide sources from Alaska driven by increasing early winter respiration from Arctic tundra. *Proceedings of the National Academy of Sciences of the United States of America*, 114(21):5361–5366, 2017.
- 530 Dalla Torre, D., Di Marco, N., Menapace, A., Avesani, D., Righetti, M., and Majone, B.: Suitability of ERA5-Land reanalysis dataset for hydrological modelling in the Alpine region, *Journal of Hydrology: Regional Studies*, 52, 101718, <https://doi.org/10.1016/j.ejrh.2024.101718>, 2024.
- 535 Druel, A., Peylin, P., Krinner, G., Ciais, P., Viovy, N., Peregon, A., Bastrikov, V., Kosykh, N., and Mironycheva-Tokareva, N.: Towards a more detailed representation of high-latitude vegetation in the global land surface model ORCHIDEE (ORCHIDEE-VEGv1.0). *Geoscientific Model Development*, 10(12):4693–4722, 2017.



540 Duel, A., Ciais, P., Krinner, G., and Peylin, P.: Modeling the Vegetation Dynamics of Northern Shrubs and Mosses in the ORCHIDEE Land Surface Model. *Journal of Advances in Modeling Earth Systems*, 11(7):2020–2035, 2019.

Ehrenfeld, J. G., Ravit, B., and Elgersma, K.: Feedback in the Plant-Soil System. *Annual Review of Environment and Resources*, 30(1):75–115, 2005.

545 Elberling, B. and Brandt, K. K.: Uncoupling of microbial CO₂ production and release in frozen soil and its implications for field studies of arctic C cycling. *Soil Biology and Biochemistry*, 35(2):263–272, 2003.

Finger, R. A., Turetsky, M. R., Kielland, K., Ruess, R. W., Mack, M. C., and Euskirchen, E. S.: Effects of permafrost thaw on nitrogen availability and plant–soil interactions in a boreal Alaskan lowland, *Journal of Ecology*, 104, 1542–1554, 550 <https://doi.org/10.1111/1365-2745.12639>, 2016.

Forbes, B. C., Fauria, M. M., and Zetterberg, P.: Russian Arctic warming and ‘greening’ are closely tracked by tundra shrub willows. *Global Change Biology*, 16(5):1542–1554, 2010.

555 Gisnås, K., Westermann, S., Schuler, T. V., Litherland, T., Isaksen, K., Boike, J., and Etzelmüller, B.: A statistical approach to represent small-scale variability of permafrost temperatures due to snow cover. *The Cryosphere*, 8(6):2063–2074, 2014.

Gisnås, K., Westermann, S., Schuler, T. V., Melvold, K., and Etzelmüller, B.: Small-scale variation of snow in a regional permafrost model. *The Cryosphere*, 10(3):1201–1215. Publisher: Copernicus GmbH, 2016.

560

Global Land Cover 2000 database. European Commission, Joint Research Centre, 2003, <https://forobs.jrc.ec.europa.eu/glc2000>

565 Gulev, S. K., Thorne, P. W., Ahn, J., Dentener, F. J., Domingues, C. M., Gerland, S., Gong, D., Kaufman, D. S., Nnamchi, H. C., Quaas, J., Rivera, J. A., Sathyendranath, S., Smith, S. L., Trewin, B., von Schuckmann, K., Vose, R. S., Allan, R., Collins, B., Turner, A., and Hawkins, E.: Changing state of the climate system, in: *Climate Change 2021: The Physical*



- Science Basis. Contribution of Working Group I to the Sixth Assessment Report of the Intergovernmental Panel on Climate Change, edited by: Masson-Delmotte, V., Zhai, P., Pirani, A., Connors, S. L., Péan, C., Berger, S., Caud, N., Chen, Y., Goldfarb, L., Gomis, M. I., Huang, M., Leitzell, K., Lonnoy, E., Matthews, J. B. R., Maycock, T. K., Waterfield, T., Yelekçi, O., Yu, R., and Zhou, B., Cambridge University Press, Cambridge, UK, 287–422, 2021.
- Guo, D., Wang, H., Romanovsky, V. E., Haywood, A. M., Pepin, N., Salzmänn, U., Sun, J., Yan, Q., Zhang, Z., Li, X., Otto-Bliesner, B. L., Feng, R., Lohmann, G., Stepanek, C., Abe-Ouchi, A., Chan, W.-L., Peltier, W. R., Chandan, D., von der Heydt, A. S., Contoux, C., Chandler, M. A., Tan, N., Zhang, Q., Hunter, S. J., and Kamae, Y.: Highly restricted near-surface permafrost extent during the mid-Pliocene warm period, *Proceedings of the National Academy of Sciences*, 120, e2301954120, <https://doi.org/10.1073/pnas.2301954120>, 2023.
- Heijmans, M. M. P. D., Magnússon, R., Lara, M. J., Frost, G. V., Myers-Smith, I. H., van Huissteden, J., Jorgenson, M. T., Fedorov, A. N., Epstein, H. E., Lawrence, D. M., and Limpens, J.: Tundra vegetation change and impacts on permafrost. *Nature Reviews Earth & Environment*, 3(1):68–84, 2022.
- Hersbach, H., Bell, B., Berrisford, P., Hirahara, S., Horányi, A., Muñoz-Sabater, J., Nicolas, J., Peubey, C., Radu, R., Schepers, D., Simmons, A., Soci, C., Abdalla, S., Abellan, X., Balsamo, G., Bechtold, P., Biavati, G., Bidlot, J., Bonavita, M., De Chiara, G., Dahlgren, P., Dee, D., Diamantakis, M., Dragani, R., Flemming, J., Forbes, R., Fuentes, M., Geer, A., Haimberger, L., Healy, S., Hogan, R. J., Hólm, E., Janisková, M., Keeley, S., Laloyaux, P., Lopez, P., Lupu, C., Radnoti, G., de Rosnay, P., Rozum, I., Vamborg, F., Villaume, S., and Thépaut, J.-N.: The ERA5 global reanalysis, *Quarterly Journal of the Royal Meteorological Society*, 146, 1999–2049, <https://doi.org/10.1002/qj.3803>, 2020.
- Hewitt, R. E., Taylor, D. L., Hollingsworth, T. N., Anderson, C. B., and Pastur, G. M.: Variable retention harvesting influences belowground plant-fungal interactions of *Nothofagus pumilio* seedlings in forests of southern Patagonia, *PeerJ*, 6, e5008, <https://doi.org/10.7717/peerj.5008>, 2018.
- Huang, J., Zhang, X., Zhang, Q., Lin, Y., Hao, M., Luo, Y., Zhao, Z., Yao, Y., Chen, X., Wang, L., Nie, S., Yin, Y., Xu, Y., and Zhang, J.: Recently amplified arctic warming has contributed to a continual global warming trend. *Nature Climate Change*, 7(12):875–879, 2017.



Jónsdóttir, I. S., Khitun, O., and Stenström, A.: Biomass and nutrient responses of a clonal tundra sedge to climate warming. *Canadian Journal of Botany*, 83(12):1608–1621, 2005.

600

Kropp, H., Loranty, M. M., Natali, S. M., Kholodov, A. L., Rocha, A. V., Myers-Smith, I., Abbot, B. W., Abermann, J., Blanc-Betes, E., Blok, D., Blume-Werry, G., Boike, J., Breen, A. L., Cahoon, S. M. P., Christiansen, C. T., Douglas, T. A., Epstein, H. E., Frost, G. V., Goeckede, M., Høye, T. T., Mamet, S. D., O'Donnell, J. A., Olefeldt, D., Phoenix, G. K., Salmon, V. G., Sannel, A. B. K., Smith, S. L., Sonnentag, O., Vaughn, L. S., Williams, M., Elberling, B., Gough, L., Hjort, J., Lafleur, P. M., Euskirchen, E. S., Heijmans, M. M., Humphreys, E. R., Iwata, H., Jones, B. M., Jorgenson, M. T., Grünberg, I., Kim, Y., Laundre, J., Mauritz, M., Michelsen, A., Schaepman-Strub, G., Tape, K. D., Ueyama, M., Lee, B.-Y., Langley, K., and Lund, M.: Shallow soils are warmer under trees and tall shrubs across Arctic and Boreal ecosystems. *Environmental Research Letters*, 16(1):015001, 2020.

610 Lawrence, D. M., Koven, C. D., Swenson, S. C., Riley, W. J., and Slater, A. G.: Permafrost thaw and resulting soil moisture changes regulate projected high-latitude CO₂ and CH₄ emissions. *Environmental Research Letters*, 10(9):094011, 2015.

Lesage, J. and Pace, R.: Introduction to Spatial Econometrics. CRC Press, Boca Raton, FL. *Introduction to Spatial Econometrics*, 1, 2009.

615

Loranty, M. M., Abbott, B. W., Blok, D., Douglas, T. A., Epstein, H. E., Forbes, B. C., Jones, B. M., Kholodov, A. L., Kropp, H., Malhotra, A., Mamet, S. D., Myers-Smith, I. H., Natali, S. M., O'Donnell, J. A., Phoenix, G. K., Rocha, A. V., Sonnentag, O., Tape, K. D., and Walker, D. A.: Reviews and syntheses: Changing ecosystem influences on soil thermal regimes in northern high-latitude permafrost regions. *Biogeosciences*, 15(17):5287–5313, 2018.

620

Luetschg, M., Stoeckli, V., Lehning, M., Haeberli, W., and Ammann, W.: Temperatures in two boreholes at Flüela Pass, Eastern Swiss Alps: the effect of snow redistribution on permafrost distribution patterns in high mountain areas. *Permafrost and Periglacial Processes*, 15(3):283–297, 2004.



- 625 Mamet, S. D., Chun, K. P., Kershaw, G. G. L., Loranty, M. M., and Peter Kershaw, G.: Recent Increases in Permafrost Thaw Rates and Areal Loss of Palsas in the Western Northwest Territories, Canada. *Permafrost and Periglacial Processes*, 28(4):619–633, 2017.
- Miner, K. R., Turetsky, M. R., Malina, E., Bartsch, A., Tamminen, J., McGuire, A. D., Fix, A., Sweeney, C., Elder, C. D.,
630 and Miller, C. E.: Permafrost carbon emissions in a changing Arctic. *Nature Reviews Earth & Environment*, 3(1):55–67, 2022.
- Morse, P., Burn, C., and Kokelj, S.: Influence of snow on near-surface ground temperatures in upland and alluvial environments of the outer Mackenzie Delta, Northwest Territories. This article is one of a series of papers published in this
635 CJES Special Issue on the theme of Fundamental and applied research on permafrost in Canada. *Canadian Journal of Earth Sciences*, 49(8):895–913, 2012.
- Muñoz Sabater, J.: ERA5-Land hourly data from 1950 to present. Copernicus Climate Change Service (C3S) Climate Data Store (CDS). DOI: [10.24381/cds.e2161bac](https://doi.org/10.24381/cds.e2161bac), 2019.
- 640 Muñoz-Sabater, J., Dutra, E., Agustí-Panareda, A., Albergel, C., Arduini, G., Balsamo, G., Boussetta, S., Choulga, M., Harrigan, S., Hersbach, H., Martens, B., Miralles, D. G., Piles, M., Rodríguez-Fernández, N. J., Zsoter, E., Buontempo, C., and Thépaut, J.-N.: ERA5-Land: a state-of-the-art global reanalysis dataset for land applications, *Earth System Science Data*, 13, 4349–4383, <https://doi.org/10.5194/essd-13-4349-2021>, 2021.
- 645 Myers-Smith, I. H., Kerby, J. T., Phoenix, G. K., Bjerke, J. W., Epstein, H. E., Assmann, J. J., John, C., Andreu-Hayles, L., Angers-Blondin, S., Beck, P. S. A., Berner, L. T., Bhatt, U. S., Bjorkman, A. D., Blok, D., Bryn, A., Christiansen, C. T., Cornelissen, J. H. C., Cunliffe, A. M., Elmendorf, S. C., Forbes, B. C., Goetz, S. J., Hollister, R. D., de Jong, R., Loranty, M. M., Macias-Fauria, M., Maseyk, K., Normand, S., Olofsson, J., Parker, T. C., Parmentier, F.-J. W., Post, E., Schaepman-Strub, G., Stordal, F., Sullivan, P. F., Thomas, H. J. D., Tømmervik, H., Treharne, R., Tweedie, C. E., Walker, D. A., Wilmking, M., and Wipf, S.: Complexity revealed in the greening of the Arctic. *Nature Climate Change*, 10(2):106–117, 2020.



655 Nitzbon, J., Schneider von Deimling, T., Aliyeva, M., Chadburn, S. E., Grosse, G., Laboor, S., Lee, H., Lohmann, G.,
Steinert, N. J., Stuenzi, S. M., Werner, M., Westermann, S., and Langer, M.: No respite from permafrost-thaw impacts in the
absence of a global tipping point, *Nat. Clim. Chang.*, 14, 573–585, <https://doi.org/10.1038/s41558-024-02011-4>, 2024.

660 Obu, J., Westermann, S., Kääb, A., and Bartsch, A.: Ground Temperature Map, 2000-2016, Northern Hemisphere
Permafrost. *Alfred Wegener Institute, Helmholtz Centre for Polar and Marine Research, Bremerhaven*. Publisher:
PANGAEA Type: dataset, 2018.

Obu, J.: How Much of the Earth's Surface is Underlain by Permafrost? *Journal of Geophysical Research: Earth Surface*,
126(5). <https://doi.org/10.1029/2021jf0006123>, 2021.

665 Ogden, E. L., Cumming, S. G., Smith, S. L., Turetsky, M. R., and Baltzer, J. L.: Permafrost thaw induces short-term increase
in vegetation productivity in northwestern Canada, *Global Change Biology*, 29, 5352–5366,
<https://doi.org/10.1111/gcb.16812>, 2023.

670 Overland, J. E., Wang, M., Walsh, J. E., and Stroeve, J. C.: Future Arctic climate changes: Adaptation and mitigation time
scales. *Earth's Future*, 2(2):68–74, 2014.

Paradis, M., Lévesque, E., and Boudreau, S.: Greater effect of increasing shrub height on winter versus summer soil
temperature. *Environmental Research Letters*, 11(8):085005, 2016.

675 Peng, X., Zhang, T., Frauenfeld, O. W., Wang, K., Cao, B., Zhong, X., Su, H., and Mu, C.: Response of seasonal soil freeze
depth to climate change across China. *The Cryosphere*, 11(3):1059–1073, 2017.

Pithan, F. and Mauritsen, T.: Arctic amplification dominated by temperature feedbacks in contemporary climate models.
Nature Geoscience, 7(3):181–184, 2014.

680



Pörtner, H.-O., D.C. Roberts, V. Masson-Delmotte, P. Zhai, M. Tignor, E. Poloczanska, K. Mintenbeck, A. Alegría, M. Nicolai, A. Okem, J. Petzold, B. Rama, N.M. Weyer (eds.)). IPCC Special Report on the Ocean and Cryosphere in a Changing Climate. Cambridge University Press, Cambridge, UK and New York, NY, USA, pp. 3–35. <https://doi.org/10.1017/9781009157964.001>, 2019

685

Rantanen, M., Karpechko, A. Y., Lipponen, A., Nordling, K., Hyvärinen, O., Ruosteenoja, K., Vihma, T., and Laaksonen, A.: The Arctic has warmed nearly four times faster than the globe since 1979. *Communications Earth & Environment*, 3(1):1–10. Number: 1, 2022.

690 Rixen, C., Wipf, S., Frei, E., and Stöckli, V.: Faster, higher, more? Past, present and future dynamics of alpine and arctic flora under climate change. *Alpine Botany*, 124(2):77–79, 2014.

Romanovsky, V. E., Sazonova, T. S., Balobaev, V. T., Shender, N. I., and Sergueev, D. O.: Past and recent changes in air and permafrost temperatures in eastern Siberia. *Global and Planetary Change*, 56(3):399–413, 2007.

695

Rößger, N., Sachs, T., Wille, C., Boike, J., and Kutzbach, L.: Seasonal increase of methane emissions linked to warming in Siberian tundra. *Nature Climate Change*, 12(11):1031–1036. Number: 11, 2022.

Schaefer, K., Lantuit, H., Romanovsky, V., Schuur, E. A. G., and Witt, R.: The impact of the permafrost carbon feedback on global climate. *Environmental Research Letters*, 2014.

700

Schuur, E. A. G., Bockheim, J., Canadell, J. G., Euskirchen, E., Field, C. B., Goryachkin, S. V., Hagemann, S., Kuhry, P., Lafleur, P. M., Lee, H., Mazhitova, G., Nelson, F. E., Rinke, A., Romanovsky, V. E., Shiklomanov, N., Tarnocai, C., Venevsky, S., Vogel, J. G., and Zimov, S. A.: Vulnerability of Permafrost Carbon to Climate Change: Implications for the Global Carbon Cycle. *BioScience*, 58(8):701–714, 2008.

705

Schuur, E. A. G., McGuire, A., Romanovsky, V. E., Schädel, C., and Mack, M.: Chapter 11: Arctic and boreal carbon. In *Second State of the Carbon Cycle Report (SOCCR2): A Sustained Assessment Report*, pages 428–468. U.S. Global Change Research Program, Washington, DC, Washington, DC : US, 2018.



710

Shaver, G. R., Bret-Harte, M. S., Jones, M. H., Johnstone, J., Gough, L., Laundre, J., and Chapin III, F. S.: Species Composition Interacts with Fertilizer to Control Long-Term Change in Tundra Productivity. *Ecology*, 82(11):3163–3181, 2001.

715 Shogren, A. J., Zarnetske, J. P., Abbott, B. W., Iannucci, F., and Bowden, W. B.: We can- not shrug off the shoulder seasons: addressing knowledge and data gaps in an Arctic headwater. 15(10):104027, 2020.

Siewert, M. B., Lantuit, H., Richter, A., and Hugelius, G.: Permafrost Causes Unique Fine-Scale Spatial Variability Across Tundra Soils, *Global Biogeochemical Cycles*, 35, e2020GB006659, <https://doi.org/10.1029/2020GB006659>, 2021.

720

Smith, S. L., Riseborough, D. W., Bonnaventure, P. P., and Duchesne, C.: An ecoregional assessment of freezing season air and ground surface temperature in the Mackenzie Valley corridor, NWT, Canada. *Cold Regions Science and Technology*, 125:152–161, 2016.

725 Smith, S. L., O'Neill, H. B., Isaksen, K., Noetzi, J., and Romanovsky, V. E.: The changing thermal state of permafrost. *Nature Reviews Earth & Environment*, 3(1):10–23, 2022.

Sturm, M., Liston, G. E., Benson, C. S., and Holmgren, J.: Characteristics and Growth of a Snowdrift in Arctic Alaska, *U.S.A. Arctic, Antarctic, and Alpine Research*, 33(3):319–329, 2001a.

730

Sturm, M., Racine, C., and Tape, K.: Increasing shrub abundance in the Arctic. *Nature*, 411(6837):546–547, 2001b.

Tikhomirov, A. B., Lesins, G., and Drummond, J. R.: Drone measurements of surface-based winter temperature inversions in the High Arctic at Eureka, *Atmospheric Measurement Techniques*, 14, 7123–7145, [https://doi.org/10.5194/amt-14-7123-](https://doi.org/10.5194/amt-14-7123-2021)
735 2021, 2021.



Villani, M., Hirst, C., du Bois d'Aische, E., Thomas, M., Lundin, E., Giesler, R., Mörtz, C.-M., and Opfergelt, S.: Lengthening of biogeochemical processes during winter in degraded permafrost soils, *Geochemical Perspectives Letters*, 34, 36–42, 2025.

740

Walvoord, M. A. and Kurylyk, B. L.: Hydrologic Impacts of Thawing Permafrost—A Review. *Vadose Zone Journal*, 15(6):vzj2016.01.0010, 2016.

745

Wang, Z., Kim, Y., Seo, H., Um, M.-J., and Mao, J.: Permafrost response to vegetation greenness variation in the Arctic tundra through positive feedback in surface air temperature and snow cover. *Environmental Research Letters*, 14(4):044024, 2019.

Wilson, J. W.: Notes on Wind and its Effects in Arctic-Alpine Vegetation. *Journal of Ecology*, 47(2):415–427, 1959.

750

Wu, J.-H., Tang, C.-S., Shi, B., Gao, L., Jiang, H.-T., and Daniels, J. L.: Effect of Ground Covers on Soil Temperature in Urban and Rural Areas. *Environmental and Engineering Geoscience*, 20(3):225–237, 2014.

Wynn, T. M. and Mostaghimi, S.: Effects of riparian vegetation on stream bank subaerial processes in southwestern Virginia, USA. *Earth Surface Processes and Landforms*, 31(4):399–413, 2006.

755

Xie, S.-P., Deser, C., Vecchi, G. A., Collins, M., Delworth, T. L., Hall, A., Hawkins, E., Johnson, N. C., Cassou, C., Giannini, A., and Watanabe, M.: Towards predictive understanding of regional climate change. *Nature Climate Change*, 5(10):921–930, 2015.

760

Ye, B., Yang, D., Zhang, Z., and Kane, D. L.: Variation of hydrological regime with permafrost coverage over Lena Basin in Siberia, *Journal of Geophysical Research: Atmospheres*, 114, <https://doi.org/10.1029/2008JD010537>, 2009.



- 765 Ylönen, M., Marttila, H., Kuzmin, A., Korpelainen, P., Kumpula, T., and Ala-Aho, P.: UAV LiDAR surveys and machine learning improves snow depth and water equivalent estimates in the boreal landscapes, *EGUsphere*, 1–33, <https://doi.org/10.5194/egusphere-2025-1297>, 2025.
- 770 Yun, H., Ciais, P., Zhu, Q., Chen, D., Zohner, C. M., Tang, J., Qu, Y., Zhou, H., Schimel, J., Zhu, P., Shao, M., Christensen, J. H., Wu, Q., Chen, A., and Elberling, B.: Changes in above- versus belowground biomass distribution in permafrost regions in response to climate warming, *Proceedings of the National Academy of Sciences*, 121, e2314036121, <https://doi.org/10.1073/pnas.2314036121>, 2024.
- Zhang, T., Heginbottom, J., Barry, R., and Brown, J.: Further statistics on the distribution of permafrost and ground ice in the Northern Hemisphere. *Polar Geography*, 24:126–131, 2000.
- 775 Zhang, T., Barry, R. G., and Haeberli, W.: Numerical simulations of the influence of the seasonal snow cover on the occurrence of permafrost at high latitudes. *Norsk Geografisk Tidsskrift - Norwegian Journal of Geography*, 55(4):261–266, 2001.
- 780 Zhang, T.: Influence of the seasonal snow cover on the ground thermal regime: An overview. *Reviews of Geophysics*, 43(4), 2005.
- Zona, D., Gioli, B., Commane, R., Lindaas, J., Wofsy, S. C., Miller, C. E., Dinardo, S. J., Dengel, S., Sweeney, C., Karion, A., Chang, R. Y.-W., Henderson, J. M., Murphy, P. C., Goodrich, J. P., Moreaux, V., Liljedahl, A., Watts, J. D., Kimball, J. S., Lipson, D. A., and Oechel, W. C.: Cold season emissions dominate the Arctic tundra methane budget, *Proceedings of the National Academy of Sciences*, 113, 40–45, <https://doi.org/10.1073/pnas.1516017113>, 2016.